Journal of proteome research

Article

Total body exposure to low-dose ionizing radiation induces long-term alterations to the liver proteome of neonatally exposed mice

Mayur Vikramrao Bakshi, Omid Azimzadeh, Zarko Barjaktarovic, Stefan J Kempf, Juliane Merl-Pham, Stefanie M Hauck, Sonja Buratovic, Per Eriksson, Michael J. Atkinson, and Soile Tapio

J. Proteome Res., **Just Accepted Manuscript** • DOI: 10.1021/pr500890n • Publication Date (Web): 09 Oct 2014

Just Accepted

Journal of Proteome Research is published by the American Chemical Society. 1155 Sixteenth Street N.W., Washington, DC 20036

Total body exposure to low-dose ionizing radiation induces long-term alterations to the liver proteome of neonatally exposed mice

Mayur V. Bakshi[1], Omid Azimzadeh[1], Zarko Barjaktarovic[1], Stefan J. Kempf[1], Juliane Merl-Pham[2], Stefanie M. Hauck[2], Sonja Buratovic[3], Per Eriksson[3], Michael J. Atkinson[1, 4], Soile Tapio[1]*

[1]Helmholtz Zentrum München, German Research Center for Environmental Health, Institute of Radiation Biology, Neuherberg, Germany

[2]Helmholtz Zentrum München, German Research Center for Environmental Health, Research Unit Protein Science, Neuherberg, Germany

[3]Department of Environmental Toxicology, Uppsala University, Uppsala, Sweden

[4]Chair of Radiation Biology, Technical University of Munich, Munich, Germany

***Corresponding author**

Soile Tapio, Helmholtz Zentrum München, German Research Center for Environmental Health, Institute of Radiation Biology, Ingolstaedter Landstrasse 1, 85764 Neuherberg, Germany

Tel.: +49 89 3187 3445; Fax: +49 89 3187 3378

E-mail address: soile.tapio@helmholtz-muenchen.de

Keywords: Low-dose ionizing radiation, liver, metabolic crosstalk, PPAR alpha, proteomics, ICPL.

Abbreviations: Gy, Gray; TCA, tricarboxylic acid; IPA, Ingenuity Pathway Analysis; CVD, cardiovascular disease; H/L, heavy to light ratio; ICPL, isotope coded protein label; LC-MS, liquid chromatography mass spectrometry; PND, post-natal day; TBI, total body irradiation; PPAR, peroxisome proliferator-activated receptor; PDH, pyruvate dehydrogenase.

ABSTRACT

Tens of thousands of people are being exposed daily to environmental low-dose gamma radiation. Epidemiological data indicate that such low radiation doses may negatively affect liver function and result in the development of liver disease. However, the biological mechanisms behind these adverse effects are unknown. The aim of this study was to investigate radiation-induced damage in the liver after low radiation doses. Neonatal male NMRI mice were exposed to total body irradiation on postnatal day 10 using acute single doses ranging from 0.02 to 1.0 Gy. Early (1 day) and late (7 months) changes in the liver proteome were tracked using isotope-coded protein label technology and quantitative mass spectrometry. Our data indicate that low and moderate radiation doses induce an immediate inhibition of the glycolysis pathway and pyruvate dehydrogenase availability in the liver. Furthermore, they lead to significant long-term alterations in lipid metabolism and increased liver inflammation accompanying inactivation of the transcription factor peroxisome proliferator-activated receptor alpha. This study contributes to the understanding of the potential risk of liver damage in populations environmentally exposed to ionizing radiation.

INTRODUCTION

Exposure to ionizing radiation is omnipresent. We are constantly exposed to cosmic radiation and to gamma-rays from naturally occurring radionuclides in the ground and building materials, food and drink.[1] In addition, accidental nuclear scenarios lead to environmental contamination of unknown level. Tens of thousands of people including children are living in polluted areas and being exposed daily to low-dose gamma radiation. Most epidemiological studies concerning radiation-induced health effects are being conducted in medically or occupationally exposed populations and very little is known about the consequences of the environmental radiation.[1]

Classically, liver has been considered as one of the radiation sensitive organs.[2] Several studies using acute high doses of radiation (> 10 Gy) have shown clear structural damage and hepatic toxicity in this organ.[3, 4] Most of these data originate from locally irradiated liver tumor patients.[3] In accordance, animal studies using single high (25 Gy) and cumulative fractionated doses (total dose of 60 Gy) have indicated macroscopically detectable scarring and changes in liver function caused by deregulation of metabolic enzymes.[5] Ionizing radiation has been shown to increase the inflammatory status of the liver.[6] Inflammatory environment promotes the development of various liver diseases such as hepatitis but also that of hepatocellular carcinoma.[7] Interestingly, the recent data of atomic bomb survivors that received only moderate to low radiation doses show significantly increased mortality due to liver cancer in this cohort.[8]

The liver is the metabolic center of the body; major metabolic activities and detoxification are performed by liver mitochondria via metabolic pathways such as lipid metabolism and TCA cycle. The early postnatal period plays a pivotal role in structural and functional development of this organ with far-reaching consequences throughout the life time;[9] it has been suggested that non-alcoholic fatty liver may have roots in the neonatal period.[10] For hepatocytes, the main cellular components of the liver, the neonatal period means a time of adaptation to the new metabolic environment, mainly due to a switch in energy substrate preference from glucose in the fetal period to fatty acids following

birth.[11] The neonatal liver undergoes several changes in its functional capacity during the early postnatal period.[12]

Previous data show that mice irradiated during the neonatal period are more susceptible to life-shortening than those exposed in the intrauterine or adult period.[13] Liver cancer is significantly induced in neonatal mice already at total body doses around 0.5 Gy.[14] The decreased capacity of the newborn liver, due to its low CYP450 content, to metabolize, detoxify, and excrete drugs[15] may be responsible for the increased susceptibility to ionizing radiation. However, very little is known about the biological mechanisms leading to radiation-induced liver damage. In particular, practically nothing is known about the dose-dependency of this damage.

The aim of the current study was to elucidate immediate and late effects on liver of low-dose ionizing radiation given at early age. For this purpose, we used NMRI mice as a model. The mice were exposed to total body irradiation (TBI) on postnatal day 10 (PND 10) using doses ranging from 0.02 to 1.0 Gy. Early (1 day) and late (7 months) changes in the liver tissue were tracked by quantitative proteomics technology. As observed previously in the heart,[16, 17] transcription factor peroxisome proliferator-activated receptor alpha (PPAR alpha) was found to play a central role in the regulation of the radiation-induced metabolic changes in the liver.

2. EXPERIMENTAL SECTION

Total body irradiation of mice

Experiments were carried out in accordance with the European Communities Council Directive of 24 November 1986 (86/609/EEC), after approval from the local ethical committees (Uppsala University and the Agricultural Research Council) and by the Swedish Committee for Ethical Experiments on Laboratory Animals.

For early effect studies the male NMRI mice (Charles River) were exposed to single acute dose of total body irradiation (TBI) at PND 10 using a Cs-137 gamma radiation source (dose rate 0.2 Gy/min) delivering doses of 0.05, 0.1, 0.5 and 1.0 Gy (The Rudbeck Laboratory, Uppsala University). For late effects the mice were exposed to a single acute dose of TBI at PND 10 using a Co-60 gamma radiation source (dose rate 0.02 Gy/min) delivering doses of 0.02, 0.1, 0.5 and 1.0 Gy (The Svedberg Laboratory, Uppsala University). An ionization chamber (Markus chamber type 23343.PTW-Freiburg) was used to validate the radiation exposure as described previously.[18] Control mice were sham-irradiated and the dose was validated as mentioned above. Control and irradiated animals were sacrificed at the age of 11 days or 7 months via cervical dislocation. Livers were excised, thoroughly rinsed in phosphate-buffered saline to remove blood, snap-frozen and stored at -80°C. In total, 60 mice were used for this study.

Isolation and extraction of whole liver proteome

Whole frozen livers were powdered in liquid nitrogen using a cooled mortar and pestle. The tissue powder was resuspended in ICPL lysis buffer containing 6 M guanidine hydrochloride (SERVA) with protease and phosphatase inhibitor cocktails (Roche Diagnostics). The lysates were stored at -20° C until analysis.

Proteomic analysis

Protein quantification and labeling

The protein concentration in the tissue lysates was determined by Bradford assay following the manufacturer's instructions (Thermo Fisher).[19]

The ICPL labeling was done as previously reported.[16] Briefly, individual protein lysates (100 µg in 100 µl of 6 M guanidine hydrochloride from each biological sample) were reduced, alkylated and labeled with the respective ICPL-reagent (SERVA) as follows: ICPL-0 was used for sham-irradiated control tissue and ICPL-6 for corresponding irradiated tissue. The heavy and light labeled replicates were

combined prior to separation using 12 % SDS gel electrophoresis and staining with colloidal Coomassie Blue solution. Three biological replicates per dose and time point were analyzed in all experiments.

LC-ESI-MS/MS analysis

After staining each SDS gel lane was cut in four equal slices and subjected to in-gel digestion with trypsin (Sigma Aldrich) as described previously.[20] The generated peptides were separated by nano-HPLC and mass spectrometric analysis was performed with an LTQ Orbitrap XL mass spectrometer (Thermo Scientific) as described before.[21] Up to ten most intense ions were selected for fragmentation in the linear ion trap and target peptides already selected for MS/MS were dynamically excluded for 60 seconds.

The MS/MS spectra were searched against the Ensembl mouse database (Version: 2.4, 56416 sequences) using the MASCOT search engine (version 2.3.02; Matrix Science) with the following parameters: a precursor mass error tolerance of 10 ppm and a fragment tolerance of 0.6 Da. One missed cleavage was allowed. Carbamidomethylation was set as the fixed modification. Oxidized methionine and ICPL-0 and ICPL-6 for lysine residues and N-termini of peptides were set as the variable modifications.

Data processing for the identification and quantitation of ICPL-duplex labeled proteins was performed using Proteome Discoverer version 1.3.0.339 (Thermo Scientific). The MASCOT node uses the ions score for an MS/MS match. MASCOT Percolator node uses algorithm to discriminate correct from incorrect peptide spectrum matches and calculates accurate statistics, such as the q-value (FDR) and posterior error probability (PEP), to improve the number of confidently identified peptides at a given false discovery rate. [22] It also assigns a statistically meaningful q-value to each PSM and the probability of the individual PSM being incorrect. The peptides passing the filter settings were grouped to the identified proteins. The proteins identified by at least 2 unique “high confidence” identified peptides in two out of three replicates were considered for further quantification. The

proteins identified by at least two unique peptides in two out of three biological replicates, and quantified with an H/L variability of less than 30%, were considered for further evaluation. Proteins identified with a single peptide were manually scrutinized and regarded as unequivocally identified if they fulfilled the following four criteria: (a) they had fragmentation spectra with a long, nearly complete y- and/or b-series; (b) all lysines were modified; (c) the numbers of lysines predicted from the mass difference of the labeled pair had to match the number of lysines in the given sequence from the search query and (d) at least one mass of a modified lysine was included in the detected partial fragment series.[23] Proteins with ratios of H/L label greater than 1.30-fold or less than 0.769-fold, and having peptide q value less than 0.01 in the Percolator high confidence peptide filter, were defined as being significantly differentially expressed.

Data deposition of proteomics experiments

The MSF files of the obtained after analyzing MS/MS spectra in Proteome Discoverer can be found under http://storedb.org/project_details.php?projectid=39.

Bioinformatics analysis

The analyses of protein-protein interaction and signaling networks were performed with two bioinformatics tools: Ingenuity Pathway Analysis (IPA) (INGENUITY System. http://www.INGENUITY.com)[24] and STRING protein database (http://string-db.org/)[25]. The protein accession numbers including the relative expression values (fold-change) of each deregulated protein were uploaded to IPA and STRING to identify possible interactions between these proteins.

Immunoblotting analysis

Immunoblotting of protein extracts from control and irradiated tissues was used to validate the proteomic data. For nuclear fraction enrichment immunoblotting was also used. Proteins were separated by 1-D PAGE gel electrophoresis and transferred to nitrocellulose membranes (GE Healthcare) using a TE 77 semidry blotting system (GE Healthcare) at 0.8 mA/cm for 1 h. Membranes

were saturated for one hour with 8% advance blocking reagent (GE Healthcare) in TBS (50 mM Tris-HCl, pH 7.6 and 150 mM NaCl) containing 0.1% Tween 20 (TBS/T). Blots were incubated overnight at 4°C with anti-tropomyosin-1 (alpha) (Abcam # ab55915), anti-desmin antibodies (Abcam # ab32362), anti-PCNA (PC10, for nuclear fraction) (SantaCruz # sc56) and anti-GAPDH (SantaCruz # sc-47724) (for nuclear fraction).

After washing three times in TBS/T, blots were incubated for one hour at room temperature with horseradish peroxidise-conjugated anti-mouse or anti-rabbit secondary antibody (Santa Cruz Biotechnology) in blocking buffer (TBS/T with 5% w/v advance blocking reagent). Immuno-detection was performed with ECL advance Western blotting detection kit (GE Healthcare). The protein bands were quantified using the total lab (TL) 100 software by integrating all pixel values in the band area after background correction. Tubulin alpha (GeneTex # GTX72360) was used for normalization as it was not significantly changed in proteomics analysis of early 1.0 Gy dose.

Pyruvate dehydrogenase activity assay

Pyruvate dehydrogenase (PDH) activity was measured using the dipstick assay kit in the control, 0.05, 0.1, 0.5 and 1.0 Gy treated liver samples from PND 11. The assay was performed following manufacturer's guidelines (Abcam # ab109882). The band intensities were quantified by using the total lab (TL) 100 software.

PPAR alpha transcription factor activity assay

Nuclear fractions from three biological replicates of control, 0.02, 0.1, 0.5 and 1.0 Gy irradiated livers after 7 months post-irradiation were extracted using NE-PER Nuclear and Cytoplasmic Extraction Kit (Thermo Scientific # 78833) and the protein concentrations in the nuclear fractions were determined by Bradford assay following the manufacturer's instructions (Thermo Fisher)[19]. Equal amounts of protein from control and irradiated samples were added on immobilized dsDNA sequence coated plates containing the peroxisome proliferator response element (PPRE). PPAR alpha was detected by addition of specific primary antibody directed against PPAR alpha. After adding the secondary

antibody the activity was measured colorimetrically according to manufacturer's guidelines (Abcam # ab133107).

Serum FFA and TG analysis

Serum of the animals 7 months post-irradiation was collected immediately after sacrifice and stored at -80° C for free fatty acid (FFA) and triglyceride (TG) quantification. Control, 0.02, 0.1, 0.5 and 1.0 Gy irradiated serum samples were analyzed. The quantification was done using BioVision colorimetric assay kits (TG cat no. # K622-100 and FFA cat no. # K612-100).

Statistical analysis

Statistical analysis was performed using Graph Pad Prism (release 4). Immunoblotting results were evaluated using unpaired Student´s t-test. Data were presented as means + standard deviation (SD) or standard error of the mean (SEM). P-values equal to or smaller than 0.05 were considered to denote statistical significance. Three biological replicates were used for all experiments.

RESULTS

Proteomics analysis

The total number of all identified and significantly deregulated proteins in each group are shown in Table 1. In the early (1 day) group the proteomic alterations showed dose dependency, the number of differentially regulated proteins being smallest at the lowest dose (0.05 Gy) and greatest at the highest dose (1.0 Gy) (Figure 1 A). On the contrary, in the late-effect group (7 months) the highest number of deregulated proteins was observed at the dose of 0.1 Gy (Figure 1 B).

The immediate radiation effect on the liver proteome indicated that the three highest doses i.e. 0.1, 0.5 and 1.0 Gy had several differentially expressed proteins in common; 12 proteins were shared between all three highest doses and 26 proteins were shared between the two highest doses (Figure

1A). Many of the shared proteins belonged to the glycolytic pathway such as dihydrolipoamide S-acetyltransferase (DLAT), aldolase A (ALDO-A), and carnitine acetyltransferase (CRAT); all of these were down-regulated. Two shared proteins were components of the mitochondrial respiratory chain complex I (NDUFV-3, NDUFV-7); both of these were down-regulated (Supplementary Table S1).

The major protein category representing the late proteome alterations was the inflammatory response, with proteins such as plasminogen and fibrinogens (FGG, FGB) being up-regulated. Proteins of the beta oxidation process were also significantly affected, with enzymes such as ACAA1A (down-regulated), and ALDH-1 (up-regulated) (Supplementary Table S2).

At both time points the common affected process was translation; proteins such as CAPRIN-1, HNRNPK, and DDX-5 were found to be commonly up-regulated. We observed persistent alterations in the liver structural proteins at the two highest doses at both time points. Structural proteins such as desmin, tropomyosin-1, and decorin were found to be down-regulated (Supplementary Tables S1c, d and S2c, d). The complete lists of significantly deregulated proteins and all identified and quantified peptides are shown in the Tables S1- S4.

Bioinformatics analysis

We analyzed the protein networks after the exposure to 1.0 Gy using the STRING software tool (Supplementary Figure S4). Both early and late time points showed an effect on the translation process. After one day of exposure, the most affected protein networks were “lipid metabolism”, “mitochondrial electron transport” and “structural proteins” (Supplementary Figure S4). The long-term effects at 7 months showed alterations in “detoxification”, “catalytic proteins” and “inflammation” (Supplementary Figure S4). The STRING analysis confirmed the results of the IPA analysis.

To study protein networks involved in the radiation response we used the Ingenuity pathway Analysis (IPA) software tool (Supplementary Figures S5-S12). The analysis showed that the most important protein clusters at the lowest doses were “hepatic system disease” (0.05 Gy, early

response) (Supplementary Figure S5) and "cellular assembly and organization" (0.02 Gy, long-term response) (Supplementary Figure S9). At higher doses (0.5 Gy, 1.0 Gy) "lipid metabolism" and "energy production" were the most significant networks both at early and late time points (Supplementary Figure S8, Supplementary Figure S11, Supplementary Figure S12)). The immediate response to the dose of 1.0 Gy was characterized by the presence of stress response proteins such as glutathione S-transferase, theta 1 (up-regulated) (Supplementary Table S1d). In the long-term effects the proteins belonging to the group "inflammatory responses" was significantly presented (Supplementary Figures S11 and S12). The transcription factor PPAR alpha was predicted to be down-regulated due to the deregulation of downstream targets such as hemopexin, fibrinogens beta and gamma, catalase and CYP2C8 at the three highest doses (0.1, 0.5, 1.0 Gy) (Figure 2).

Immunoblotting analysis

Western blotting analysis was done to validate the proteomics data. Both desmin and tropomyosin-1 showed significant down-regulation at PND11 (1.0 Gy) (Figure 3 and Supplementary Figure S1) which was in good agreement with our proteomics data. The enrichment of nuclear fraction from irradiated live tissue was confirmed also using immunoblotting (Supplementary Figure S2).

Pyruvate dehydrogenase assay

In order to verify the down-regulation of the pyruvate complex and pyruvate kinase (PDK) that was indicated in the proteome changes at the early time point, we tested the activity of pyruvate dehydrogenase one day after the radiation exposure. It showed significant reduction by more than two-fold at 0.5 and 1.0 Gy but not at lower doses (Figure 4 and Supplementary Figure S3). This supported our proteomics data showing the significantly decreased expression of several pyruvate dehydrogenase subunits and pyruvate kinase at 0.5 and 1.0 Gy (Supplementary Tables S1c and S1d).

PPAR alpha activity assay

To confirm the prediction of PPAR alpha inactivation by IPA software (Figure 2), the activity of PPAR alpha was measured from nuclear extracts at the late time point (7 months). A significant dose-dependent decrease in the activity of this transcription factor was observed, starting from the dose of 0.1 Gy (Figure 5A).

Serum FFA and TG analysis

As PPAR alpha is well known to control the free fatty acid (FFA) and triglyceride (TG) homeostasis in serum, we measured the serum concentrations of FFA and TG in control, 0.02 Gy, 0.1Gy, 0.5 Gy and 1.0 Gy irradiated animals (7 months post-irradiation). The amount of FFA was found to be significantly elevated in the serum of irradiated mice at doses of 0.5 Gy and 1.0 Gy but not at lower doses. In contrast, the level of TG showed significant decrease at 0.5 Gy and 1.0Gy but not at lower doses (Figure. 5B and 5C).

DISCUSSION

In this study, we have investigated early and late alterations in biological pathways triggered by low and moderate doses of total body ionizing radiation on the developing mouse liver. We show that doses as low as 0.1 Gy were able to inactivate PPAR alpha, a key regulator of hepatic fat oxidation, in a persistent manner.

Early radiation effects one day after irradiation

As an early radiation-induced metabolic consequence the expression of pyruvate kinase isozymes (PKM) and pyruvate dehydrogenase (PDH) were found significantly down-regulated at all doses (Supplementary Table S1). As PKMs catalyze the final step in the glycolytic pathway producing pyruvate and ATP in the presence of oxygen, their down-regulation would result in less energy production through glycolysis but also less pyruvate, the main substrate of the citric acid cycle. Pyruvate does not act only as energy substrate but functions also as a scavenger of hydrogen

peroxide[26] and its reduced level may result in increased oxidative stress in irradiated liver. The reduced level of PDH, transforming pyruvate into acetyl-CoA, was accompanied by down-regulation of the PDH activity (Figure 4). It has been shown previously that down-regulation of PDH in liver is associated with increased insulin sensitivity[27], which may decrease metabolic flexibility of the liver, primarily between glucose and fatty acid oxidation.[28]

We observed an immediate effect on the glycolytic pathway with many of its proteins (DLAT, ALDO-A, CRAT) being down-regulated. Also from early on, some enzymes of the lipid metabolism, such as peroxisomal acyl-coenzyme A oxidase 1 (ACOX1) and peroxisomal acyl-coenzyme A oxidase 2 (ACOX2) were found to be deregulated. ACOX1 showed radiation-induced down-regulation whereas ACOX2 was up-regulated. ACOX1 is the first and rate-limiting enzyme of the inducible peroxisomal beta-oxidation system[29, 30] Its gene expression is positively regulated by PPAR alpha[31] and shRNA-mediated PPAR alpha gene knockdown in primary human hepatocytes decreased expression levels of Acox1 by more than 50%.[32] Mice lacking the Acox1 gene develop hepatocellular carcinomas in 100% of animals between 10 and 15 months due to constitutive overexpression of PPAR alpha.[29]

Some mitochondrial electron transport chain proteins, all belonging to the respiratory Complex I, were also found to be down-regulated (Supplementary Tables S1c and S1d). In accordance with previous data[33] we found a decrease in the level of aconitase, a key enzyme in energy metabolism in mitochondria. As aconitase is a sensitive target of reactive oxygen species and its loss limits citric acid cycle activity and mitochondrial respiratory capacity *in vivo*[33] this may indicate an early mitochondrial dysfunction and increased production of reactive oxygen species (ROS).[34, 35] Data from animal studies indicate that neonatal liver mitochondria are very sensitive to oxidative stress.[36] Oxidative stress is considered as the major reason for many metabolic disorders.[37-39]

In addition, an immediate effect of irradiation was seen in the down-regulation of the expression of many structural proteins of the cytoskeleton and connective tissue (plectin, catenin, decorin, collagen, desmin, tropomyosin). The levels of desmin, and tropomyosin-1 were found to be down-

regulated using both proteomics and immunoblotting. In hepatocytes, tropomyosin plays a role in stabilizing actin filaments.[40] The expression of desmin has been exclusively associated to hepatic stellate cells in the liver.[41] These changes indicate a rapid radiation-induced proteomic remodeling of the liver tissue.

Late PPAR alpha- mediated metabolic alterations after low to moderate radiation doses

Based on our proteomics data seven months post-irradiation PPAR alpha was predicted as deactivated, as the expression of many of the target enzymes in the lipid metabolism such as ACOX1 and ACAA1 were down-regulated whilst inflammatory response proteins such as fibrinogens and hemopexin were found up-regulated (Figure 2). Therefore, we measured the activity of PPAR alpha using nuclear extracts, and found a clear decrease in the PPAR alpha activity in the irradiated livers, even at a dose as low as 0.1 Gy (Figure 5A). The deactivation of PPAR alpha can be accomplished by both ligand-dependent and ligand-independent mechanisms.[42, 43] Unlike in the heart,[16] we did not find changes in the total or phosphorylated form of PPAR alpha in the irradiated liver (data not shown). Instead, persistent increase in oxidative stress may contribute to the deactivation of PPAR alpha as suggested by Azimzadeh et al.[17]

One of the hallmarks of inactivated PPAR alpha is its inability to use free fatty acids (FFA) for energy production.[44] In accordance with this we found elevated levels of FFA in the serum of irradiated animals (0.5 and 1.0 Gy) (Figure. 5B and 5C). In contrast, serum triglyceride (TG) levels in the irradiated mice were found decreased. The decreased levels of serum TG may result from the increased cardiac PPAR alpha activity in these animals,[16] as overexpression of PPAR alpha in the heart induces triglyceride accumulation in cardiomyocytes.[16, 45] Our results and previous data suggest that there is an intensive crosstalk between heart and liver, especially in the neonatal phase.[46]

Late increase in the level of cytochrome CYP450 enzymes in irradiated liver

Cytochrome P450 is a large and diverse group of enzymes that catalyze the oxidation of organic substances. We found up-regulation of several types of CYP450 but especially Cyp2E1 that was

persistently up-regulated at doses of 0.1, 0.5 and 1.0 Gy (Supplementary Tables S2b, c and d). It has been shown previously that the expression of CYP2E1 was immediately induced after exposure to gamma rays (3 Gy) in rat liver.[33] A dose-dependent increase of CYP2E1 was also shown after fast neutron irradiation in mouse liver.[47] It has been demonstrated that in conditions with increased oxidative stress Cyp2E1 plays an important role in the induction of mitochondrial dysfunction.[48]

CONCLUSIONS

These data suggest a long-term radiation-induced but dose-dependent inactivation of transcription factor PPAR alpha in liver, associated with mitochondrial dysfunction and increased oxidative stress. Total body radiation doses as low as 0.1 Gy given to neonatal mice resulted in both immediate and persistent adverse effects on the metabolic pathways. Although doses lower than 0.1 Gy caused long-term alterations in the liver proteome, these very low doses did not result in significant changes in any of the functional assays performed in this study. In contrast, exposure to the dose of 0.5 Gy resulted in alterations in all endpoints that were investigated. Although “absence of evidence is not evidence of absence” it must be concluded that this study gives no support to long-term liver damage at doses lower than 0.1 Gy in a mouse model. Together with our previous data on the cardiac effects in these animals these results underscore the importance of systemic effects after low radiation doses relevant in environmental exposure situations.

ACKNOWLEDGMENTS

We thank Stefanie Winkler for her technical assistance.

Figure legends

Figure 1 Venn diagram showing the number of significantly deregulated and shared proteins affected in all irradiated samples at 1 day (A) and 7 month post-irradiation (B).

Figure 2 Ingenuity Pathway Analysis networks showing transcriptional factor PPAR alpha as an upstream regulator. PPAR alpha is predicted deactivated in all networks at long-term time point. The proteins indicated in red are up-regulated and those indicated in green are down-regulated. Three biological replicates were used in all experiments. ACACA, acetyl-Coenzyme A carboxylase alpha; ACOX1, peroxisomal acyl-coenzyme A oxidase 1; ACCL5, acyl-CoA synthetase long-chain family member 5; ASS1, argininosuccinate synthetase 1; CAT, catalase; FGA, fibrinogen alpha; FGB, fibrinogen beta; FGG, fibrinogen gamma; PBLD1, phenazine biosynthesis-like protein domain containing 1; UGT1A9, UDP glucuronosyltransferase 1 family, polypeptide A9; CS, citrate synthase; C3, Complement C3 precursor; HPX, hemopexin; PCK1, phosphoenolpyruvate carboxykinase 1; TPP1, tripeptidyl peptidase I; ACAA1, acetyl-Coenzyme A acyltransferase 1A; CPT1A, carnitine palmitoyltransferase 1a; PPARA, peroxisome proliferator-activated receptor alpha.

Figure 3 Immunoblot validation of proteomic results (1.0 Gy; PND 11) using anti-desmin and anti-tropomyosin-1 antibodies. A significant down-regulation of the levels of desmin and tropomyosin-1 are shown. Columns represent the average ratios with standard deviation (SD) of relative protein expression in control and 1.0 Gy (PND 11) irradiated samples after background correction and normalization to tubulin alpha. (Unpaired Student´s t-test; *p ≤0.05; n=3).

Figure 4 Columns representing n fold-changes with their corresponding standard error of the means (SEM) from the biological replicates to evaluate liver pyruvate dehydrogenase (PDH) activity in the control, 0.05, 0.1, 0.5 and 1.0 Gy dose at PND11; statistical analysis was performed with unpaired Student´s t-test; *p ≤0.05; ns, not significant; n=3; data origin from two independent experiments to evaluate PDH activity at 1.0 and lower doses (0.5 Gy, 0.1 Gy and 0.05 Gy) versus the same respective controls.

Figure 5 (A) Columns representing quantification of PPAR alpha activity assay in liver of control, 0.02, 0.1, 0.5 and 1.0 Gy samples 7 months post irradiation (AU; arbitrary unit). Columns representing quantification of triglycerides **(B)** and free fatty acid **(C)** in the serum samples of control, 0.02, 0.1, 0.5 and 1.0 Gy samples 7 month post irradiation (Unpaired Student´s t-test; *p ≤0.05; **p ≤0.01; n=3).

SUPPORTING INFORMATION

Supporting Information Available: Description of the material. This material is available free of charge via the Internet at http://pubs.acs.org.

Supplementary Table and Figure Legends

Supplementary Table S1 (a-d). Significantly deregulated proteins in irradiated samples (Postnatal day 11)

Supplementary Table S2 (a-d). Significantly deregulated proteins in irradiated samples (7 months post-irradiation).

Supplementary Table S3. All peptides identified and quantified after high confidence peptide filtering (a-d) after day 1.

Supplementary Table S4. All peptides identified and quantified after high confidence peptide filtering (a-d) after 7 months.

Supplementary Figure S1: Immunoblotting images of different proteins expressed after a dose of 1.0 Gy.

Supplementary Figure S2: Immunoblotting image showing enrichment of nuclear fraction from irradiated liver tissue.

Supplementary Figure S3: Dip-stick assay showing relative abundance of Pyruvate dehydrogenase in control, 0.05, 0.1, 0.5 and 1.0 Gy irradiated livers (Post-natal day 11).

Supplementary Figure S4: STRING protein networks showing comparison between different classes of proteins significantly deregulated at the dose of 1.0 Gy at PND 11 and 7 months post irradiation time points.

Supplementary Figure S5: IPA summary analysis of 0.05 Gy early (PND11) liver analysis

Supplementary Figure S6: IPA summary analysis of 0.1 Gy early (PND11) liver analysis

Supplementary Figure S7: IPA summary analysis of 0.5 Gy early (PND11) liver analysis

Supplementary Figure S8: IPA summary analysis of 1.0 Gy early (PND11) liver analysis

Supplementary Figure S9: IPA summary analysis of 0.02 Gy long-term liver analysis

Supplementary Figure S10: IPA summary analysis of 0.1 Gy long-term liver analysis

Supplementary Figure S11: IPA summary analysis of 0.5 Gy long-term liver analysis

Supplementary Figure S12: IPA summary analysis of 1.0 Gy long-term liver analysis

The authors declare no competing financial interest.

REFERENCES

1. Wakeford, R., The cancer epidemiology of radiation. *Oncogene* **2004,** 23, (38), 6404-28.

2. Stryker, J. A., Science to practice: why is the liver a radiosensitive organ? *Radiology* **2007,** 242, (1), 1-2.

3. Liu, W.; Haley, B. M.; Kwasny, M. J.; Li, J. J.; Grdina, D. J.; Paunesku, T.; Woloschak, G. E., The effects of radiation and dose-fractionation on cancer and non-tumor disease development. *Int J Environ Res Public Health* **2012,** 9, (12), 4688-703.

4. Dawson, L. A.; Normolle, D.; Balter, J. M.; McGinn, C. J.; Lawrence, T. S.; Ten Haken, R. K., Analysis of radiation-induced liver disease using the Lyman NTCP model. *Int J Radiat Oncol Biol Phys* **2002,** 53, (4), 810-21.

5. Rave-Fränk, M.; Malik, I.; Christiansen, H.; Naz, N.; Sultan, S.; Amanzada, A.; Blaschke, M.; Cameron, S.; Ahmad, S.; Hess, C.; Ramadori, G.; Moriconi, F., Rat model of fractionated (2 Gy/day) 60 Gy irradiation of the liver: long-term effects. *Radiation and Environmental Biophysics* **2013,** 52, (3), 321-338.

6. Gridley, D. S.; Mao, X. W.; Cao, J. D.; Bayeta, E. J.; Pecaut, M. J., Protracted low-dose radiation priming and response of liver to acute gamma and proton radiation. *Free Radic Res* **2013,** 47, (10), 811-20.

7. Marra, F.; Tacke, F., Roles for Chemokines in Liver Disease. *Gastroenterology* **2014**.

8. Ozasa, K.; Shimizu, Y.; Suyama, A.; Kasagi, F.; Soda, M.; Grant, E. J.; Sakata, R.; Sugiyama, H.; Kodama, K., Studies of the mortality of atomic bomb survivors, Report 14, 1950-2003: an overview of cancer and noncancer diseases. *Radiat Res* **2012,** 177, (3), 229-43.

9. Kanamura, S.; Kanai, K.; Watanabe, J., Fine structure and function of hepatocytes during development. *J Electron Microsc Tech* **1990,** 14, (2), 92-105.

10. Beath, S. V., Hepatic function and physiology in the newborn. *Semin Neonatol* **2003,** 8, (5), 337-46.

11. Lehman, J. J.; Kelly, D. P., Transcriptional activation of energy metabolic switches in the developing and hypertrophied heart. *Clin Exp Pharmacol Physiol* **2002,** 29, (4), 339-45.

12. Grijalva, J.; Vakili, K., Neonatal liver physiology. *Semin Pediatr Surg* **2013,** 22, (4), 185-9.

13. Sasaki, S.; Fukuda, N., Temporal variation of excess mortality rate from solid tumors in mice irradiated at various ages with gamma rays. *J Radiat Res* **2005,** 46, (1), 1-19.

14. Sasaki, S.; Fukuda, N., Dose-response relationship for induction of solid tumors in female B6C3F1 mice irradiated neonatally with a single dose of gamma rays. *J Radiat Res* **1999,** 40, (3), 229-41.

15. Faa, G.; Ekstrom, J.; Castagnola, M.; Gibo, Y.; Ottonello, G.; Fanos, V., A developmental approach to drug-induced liver injury in newborns and children. *Curr Med Chem* **2012,** 19, (27), 4581-94.

16. Bakshi, M. V.; Barjaktarovic, Z.; Azimzadeh, O.; Kempf, S. J.; Merl, J.; Hauck, S. M.; Eriksson, P.; Buratovic, S.; Atkinson, M. J.; Tapio, S., Long-term effects of acute low-dose ionizing radiation on the neonatal mouse heart: a proteomic study. *Radiat Environ Biophys* **2013,** 52, (4), 451-61.

17. Azimzadeh, O.; Sievert, W.; Sarioglu, H.; Yentrapalli, R.; Barjaktarovic, Z.; Sriharshan, A.; Ueffing, M.; Janik, D.; Aichler, M.; Atkinson, M. J.; Multhoff, G.; Tapio, S., PPAR Alpha: A Novel Radiation Target in Locally Exposed Mus musculus Heart Revealed by Quantitative Proteomics. *J Proteome Res* **2013,** 12, (6), 2700-14.

18. Eriksson, P.; Fischer, C.; Stenerlow, B.; Fredriksson, A.; Sundell-Bergman, S., Interaction of gamma-radiation and methyl mercury during a critical phase of neonatal brain development in mice exacerbates developmental neurobehavioural effects. *Neurotoxicology* **2010,** 31, (2), 223-9.

19. Bradford, M. M., A rapid and sensitive method for the quantitation of microgram quantities of protein utilizing the principle of protein-dye binding. *Anal Biochem* **1976,** 72, 248-54.

20. Merl, J.; Ueffing, M.; Hauck, S. M.; von Toerne, C., Direct comparison of MS-based label-free and SILAC quantitative proteome profiling strategies in primary retinal Muller cells. *Proteomics* **2012,** 12, (12), 1902-11.

21. Hauck, S. M.; Dietter, J.; Kramer, R. L.; Hofmaier, F.; Zipplies, J. K.; Amann, B.; Feuchtinger, A.; Deeg, C. A.; Ueffing, M., Deciphering membrane-associated molecular processes in target tissue of autoimmune uveitis by label-free quantitative mass spectrometry. *Mol Cell Proteomics* **2010,** 9, (10), 2292-305.

22. Brosch, M.; Yu, L.; Hubbard, T.; Choudhary, J., Accurate and sensitive peptide identification with Mascot Percolator. *J Proteome Res* **2009,** 8, (6), 3176-81.

23. Sarioglu, H.; Brandner, S.; Jacobsen, C.; Meindl, T.; Schmidt, A.; Kellermann, J.; Lottspeich, F.; Andrae, U., Quantitative analysis of 2,3,7,8-tetrachlorodibenzo-p-dioxin-induced proteome alterations in 5L rat hepatoma cells using isotope-coded protein labels. *Proteomics* **2006,** 6, (8), 2407-21.

24. Mayburd, A. L.; Martlinez, A.; Sackett, D.; Liu, H.; Shih, J.; Tauler, J.; Avis, I.; Mulshine, J. L., Ingenuity network-assisted transcription profiling: Identification of a new pharmacologic mechanism for MK886. *Clin Cancer Res* **2006,** 12, (6), 1820-7.

25. Szklarczyk, D.; Franceschini, A.; Kuhn, M.; Simonovic, M.; Roth, A.; Minguez, P.; Doerks, T.; Stark, M.; Muller, J.; Bork, P.; Jensen, L. J.; von Mering, C., The STRING database in 2011: functional interaction networks of proteins, globally integrated and scored. *Nucleic Acids Res* **2011,** 39, (Database issue), D561-8.

26. Eghbal, M. A.; Pennefather, P. S.; O'Brien, P. J., H2S cytotoxicity mechanism involves reactive oxygen species formation and mitochondrial depolarisation. *Toxicology* **2004,** 203, (1-3), 69-76.

27. Choi, C. S.; Ghoshal, P.; Srinivasan, M.; Kim, S.; Cline, G.; Patel, M. S., Liver-specific pyruvate dehydrogenase complex deficiency upregulates lipogenesis in adipose tissue and improves peripheral insulin sensitivity. *Lipids* **2010,** 45, (11), 987-95.

28. Zhang, S.; Hulver, M. W.; McMillan, R. P.; Cline, M. A.; Gilbert, E. R., The pivotal role of pyruvate dehydrogenase kinases in metabolic flexibility. *Nutr Metab (Lond)* **2014,** 11, (1), 10.

29. Meyer, K.; Jia, Y.; Cao, W. Q.; Kashireddy, P.; Rao, M. S., Expression of peroxisome proliferator-activated receptor alpha, and PPARalpha regulated genes in spontaneously developed hepatocellular carcinomas in fatty acyl-CoA oxidase null mice. *Int J Oncol* **2002,** 21, (6), 1175-80.

30. Meyer, K.; Lee, J. S.; Dyck, P. A.; Cao, W. Q.; Rao, M. S.; Thorgeirsson, S. S.; Reddy, J. K., Molecular profiling of hepatocellular carcinomas developing spontaneously in acyl-CoA oxidase deficient mice: comparison with liver tumors induced in wild-type mice by a peroxisome proliferator and a genotoxic carcinogen. *Carcinogenesis* **2003,** 24, (5), 975-84.

31. Varanasi, U.; Chu, R.; Huang, Q.; Castellon, R.; Yeldandi, A. V.; Reddy, J. K., Identification of a peroxisome proliferator-responsive element upstream of the human peroxisomal fatty acyl coenzyme A oxidase gene. *J Biol Chem* **1996,** 271, (4), 2147-55.

32. Klein, K.; Thomas, M.; Winter, S.; Nussler, A. K.; Niemi, M.; Schwab, M.; Zanger, U. M., PPARA: a novel genetic determinant of CYP3A4 in vitro and in vivo. *Clin Pharmacol Ther* **2012,** 91, (6), 1044-52.

33. Chung, H. C.; Kim, S. H.; Lee, M. G.; Cho, C. K.; Kim, T. H.; Lee, D. H.; Kim, S. G., Mitochondrial dysfunction by gamma-irradiation accompanies the induction of cytochrome P450 2E1 (CYP2E1) in rat liver. *Toxicology* **2001,** 161, (1-2), 79-91.

34. Drose, S.; Brandt, U., The mechanism of mitochondrial superoxide production by the cytochrome bc1 complex. *J Biol Chem* **2008,** 283, (31), 21649-54.

35. Barjaktarovic, Z.; Schmaltz, D.; Shyla, A.; Azimzadeh, O.; Schulz, S.; Haagen, J.; Dörr, W.; Sarioglu, H.; Schäfer, A.; Atkinson, M. J.; Zischka, H.; Tapio, S., Radiation–induced Signaling Results in Mitochondrial Impairment in Mouse Heart at 4 Weeks after Exposure to X-rays. *PLoS One* **2011,** 6, (12), e27811.

36. Lazarin Mde, O.; Ishii-Iwamoto, E. L.; Yamamoto, N. S.; Constantin, R. P.; Garcia, R. F.; da Costa, C. E.; Vitoriano Ade, S.; de Oliveira, M. C.; Salgueiro-Pagadigorria, C. L., Liver mitochondrial function and redox status in an experimental model of non-alcoholic fatty liver disease induced by monosodium L-glutamate in rats. *Exp Mol Pathol* **2011,** 91, (3), 687-94.

37. Barjaktarovic, Z.; Schmaltz, D.; Shyla, A.; Azimzadeh, O.; Schulz, S.; Haagen, J.; Dorr, W.; Sarioglu, H.; Schafer, A.; Atkinson, M. J.; Zischka, H.; Tapio, S., Radiation-induced signaling results in mitochondrial impairment in mouse heart at 4 weeks after exposure to X-rays. *PLoS One* **2011,** 6, (12), e27811.

38. Barjaktarovic, Z.; Shyla, A.; Azimzadeh, O.; Schulz, S.; Haagen, J.; Dorr, W.; Sarioglu, H.; Atkinson, M. J.; Zischka, H.; Tapio, S., Ionising radiation induces persistent alterations in the cardiac mitochondrial function of C57BL/6 mice 40 weeks after local heart exposure. *Radiother Oncol* **2013,** 106, (3), 404-10.

39. Johnson, W. M.; Wilson-Delfosse, A. L.; Mieyal, J. J., Dysregulation of Glutathione Homeostasis in Neurodegenerative Diseases. *Nutrients* **2012,** 4, (10), 1399-440.

40. Yokoyama, Y.; Kuramitsu, Y.; Takashima, M.; Iizuka, N.; Toda, T.; Terai, S.; Sakaida, I.; Oka, M.; Nakamura, K.; Okita, K., Proteomic profiling of proteins decreased in hepatocellular carcinoma from patients infected with hepatitis C virus. *Proteomics* **2004,** 4, (7), 2111-6.

41. Nitou, M.; Ishikawa, K.; Shiojiri, N., Immunohistochemical analysis of development of desmin-positive hepatic stellate cells in mouse liver. *J Anat* **2000,** 197 Pt 4, 635-46.

42. Lazennec, G.; Canaple, L.; Saugy, D.; Wahli, W., Activation of peroxisome proliferator-activated receptors (PPARs) by their ligands and protein kinase A activators. *Mol Endocrinol* **2000,** 14, (12), 1962-75.

43. Vanden Heuvel, J. P.; Kreder, D.; Belda, B.; Hannon, D. B.; Nugent, C. A.; Burns, K. A.; Taylor, M. J., Comprehensive analysis of gene expression in rat and human hepatoma cells exposed to the peroxisome proliferator WY14,643. *Toxicol Appl Pharmacol* **2003,** 188, (3), 185-98.

44. Francis, G. A.; Annicotte, J. S.; Auwerx, J., PPAR-alpha effects on the heart and other vascular tissues. *Am J Physiol Heart Circ Physiol* **2003,** 285, (1), H1-9.

45. Palomer, X.; Salvado, L.; Barroso, E.; Vazquez-Carrera, M., An overview of the crosstalk between inflammatory processes and metabolic dysregulation during diabetic cardiomyopathy. *Int J Cardiol* **2013,** 168, (4), 3160-72.

46. Magida, J. A.; Leinwand, L. A., Metabolic crosstalk between the heart and liver impacts familial hypertrophic cardiomyopathy. *EMBO Mol Med* **2014,** 6, (4), 482-95.

47. Jeong, W. I.; Do, S. H.; Kim, T. H.; Jeong, D. H.; Hong, I. H.; Ki, M. R.; Kwak, D. M.; Lee, S. S.; Jee, Y. H.; Kim, S. B.; Jeong, K. S., Acute effects of fast neutron irradiation on mouse liver. *J Radiat Res* **2007,** 48, (3), 233-40.

48. Qi, X. M.; Miao, L. L.; Cai, Y.; Gong, L. K.; Ren, J., ROS generated by CYP450, especially CYP2E1, mediate mitochondrial dysfunction induced by tetrandrine in rat hepatocytes. *Acta Pharmacol Sin* **2013,** 34, (9), 1229-36.

Table 1 The numbers of all proteins identified and significantly deregulated in this study. The different doses and time points are indicated.

Dose in Gy	1 day post IR		7 months post IR	
	Total identified	Significantly deregulated	Total identified	Significantly deregulated
0.05/0.02	1683	40	1669	42
0.1	1768	56	1528	76
0.5	1698	74	1484	60
1.0	1664	77	1440	64

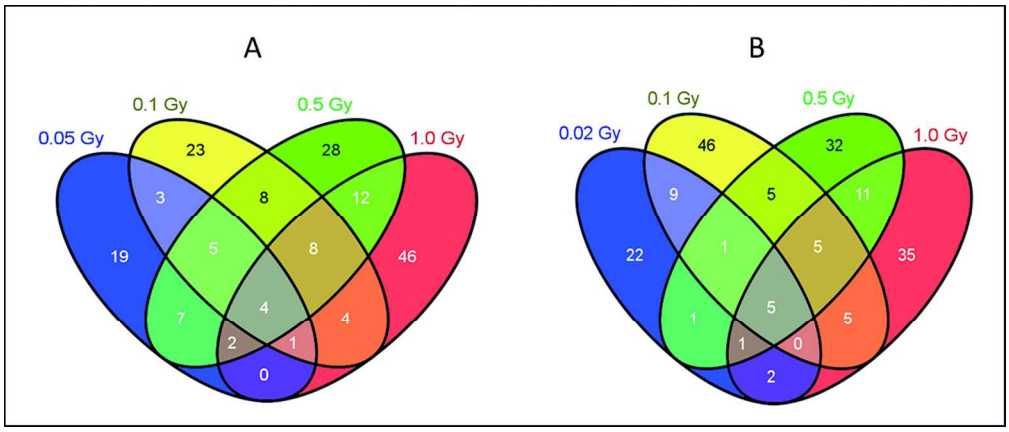

Figure 1 Venn diagram showing the number of significantly deregulated and shared proteins affected in all irradiated samples at 1 day (A) and 7 month post-irradiation (B).
170x71mm (300 x 300 DPI)

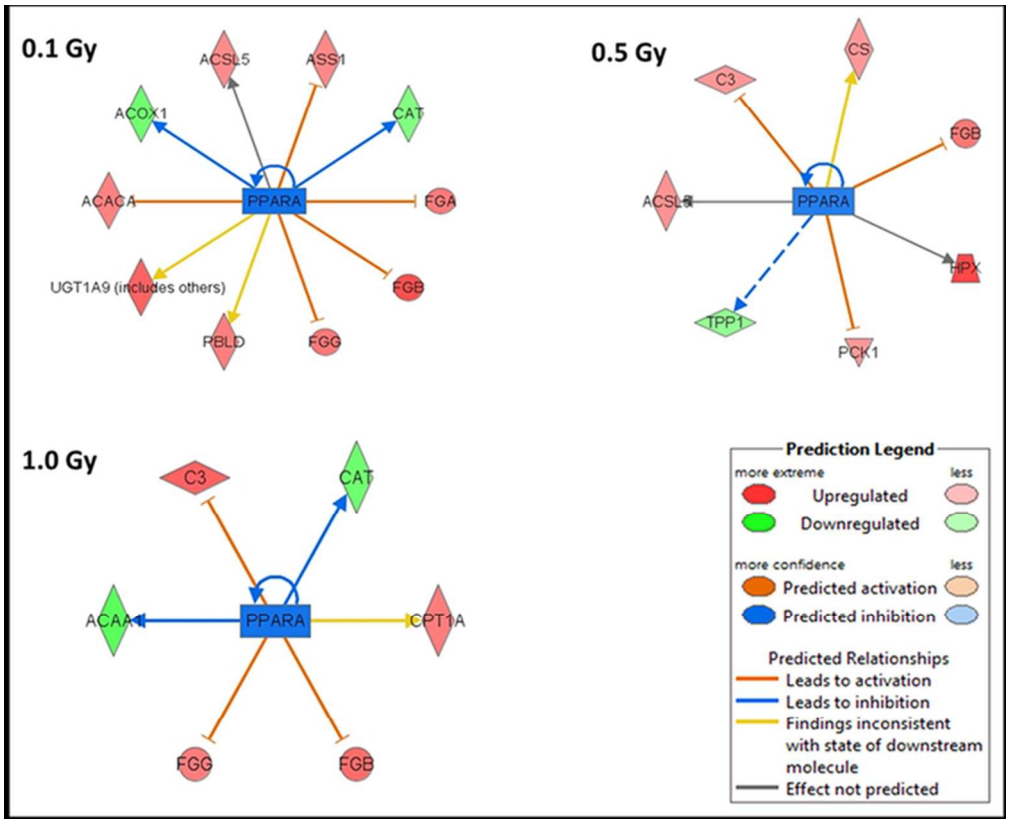

Figure 2 Ingenuity Pathway Analysis networks showing transcriptional factor PPAR alpha as an upstream regulator. PPAR alpha is predicted deactivated in all networks at long-term time point. The proteins indicated in red are up-regulated and those indicated in green are down-regulated. Three biological replicates were used in all experiments. ACACA, acetyl-Coenzyme A carboxylase alpha; ACOX1, peroxisomal acyl-coenzyme A oxidase 1; ACCL5, acyl-CoA synthetase long-chain family member 5; ASS1, argininosuccinate synthetase 1; CAT, catalase; FGA, fibrinogen alpha; FGB, fibrinogen beta; FGG, fibrinogen gamma; PBLD1, phenazine biosynthesis-like protein domain containing 1; UGT1A9, UDP glucuronosyltransferase 1 family, polypeptide A9; CS, citrate synthase; C3, Complement C3 precursor; HPX, hemopexin; PCK1, phosphoenolpyruvate carboxykinase 1; TPP1, tripeptidyl peptidase I; ACAA1, acetyl-Coenzyme A acyltransferase 1A; CPT1A, carnitine palmitoyltransferase 1a; PPARA, peroxisome proliferator-activated receptor alpha.
64x52mm (300 x 300 DPI)

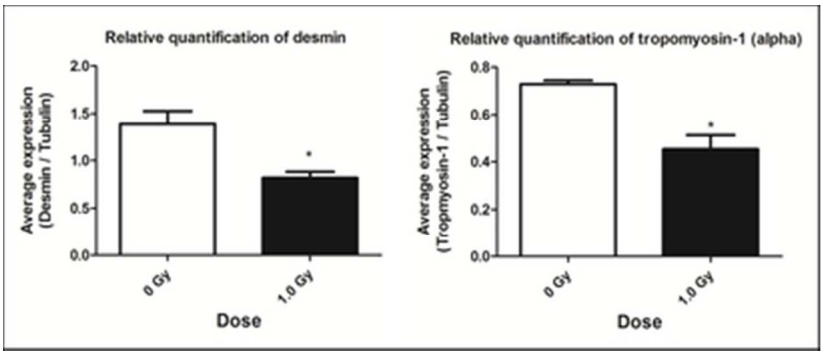

Figure 3 Immunoblot validation of proteomic results (1.0 Gy; PND 11) using anti-desmin and anti-tropomyosin-1 antibodies. A significant down-regulation of the levels of desmin and tropomyosin-1 are shown. Columns represent the average ratios with standard deviation (SD) of relative protein expression in control and 1.0 Gy (PND 11) irradiated samples after background correction and normalization to tubulin alpha. (Unpaired Student´s t-test; *p ≤0.05; n=3).
17x7mm (600 x 600 DPI)

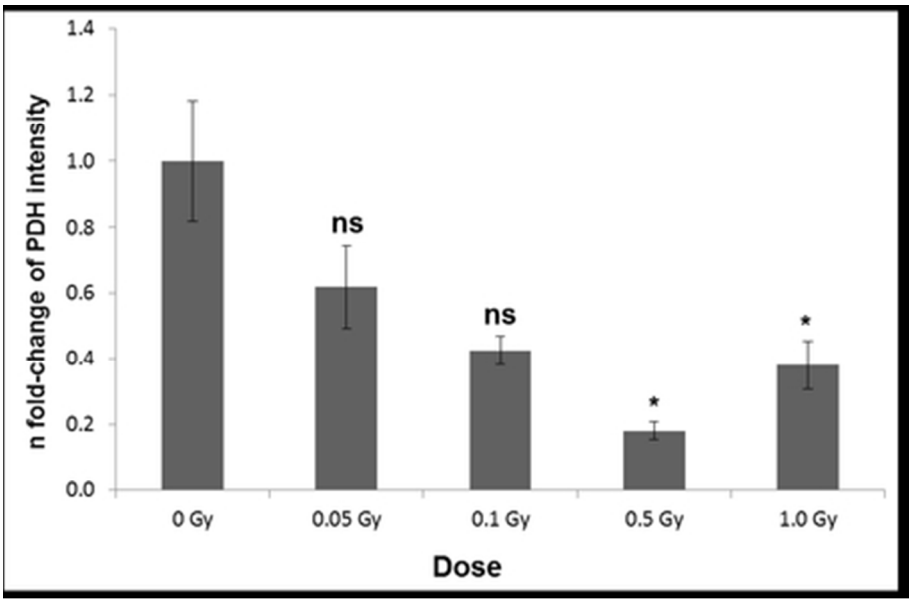

Figure 4 Columns representing n fold-changes with their corresponding standard error of the means (SEM) from the biological replicates to evaluate liver pyruvate dehydrogenase (PDH) activity in the control, 0.05, 0.1, 0.5 and 1.0 Gy dose at PND11; statistical analysis was performed with unpaired Student´s t-test; *p ≤0.05; ns, not significant; n=3; data origin from two independent experiments to evaluate PDH activity at 1.0 and lower doses (0.5 Gy, 0.1 Gy and 0.05 Gy) versus the same respective controls.
19x12mm (600 x 600 DPI)

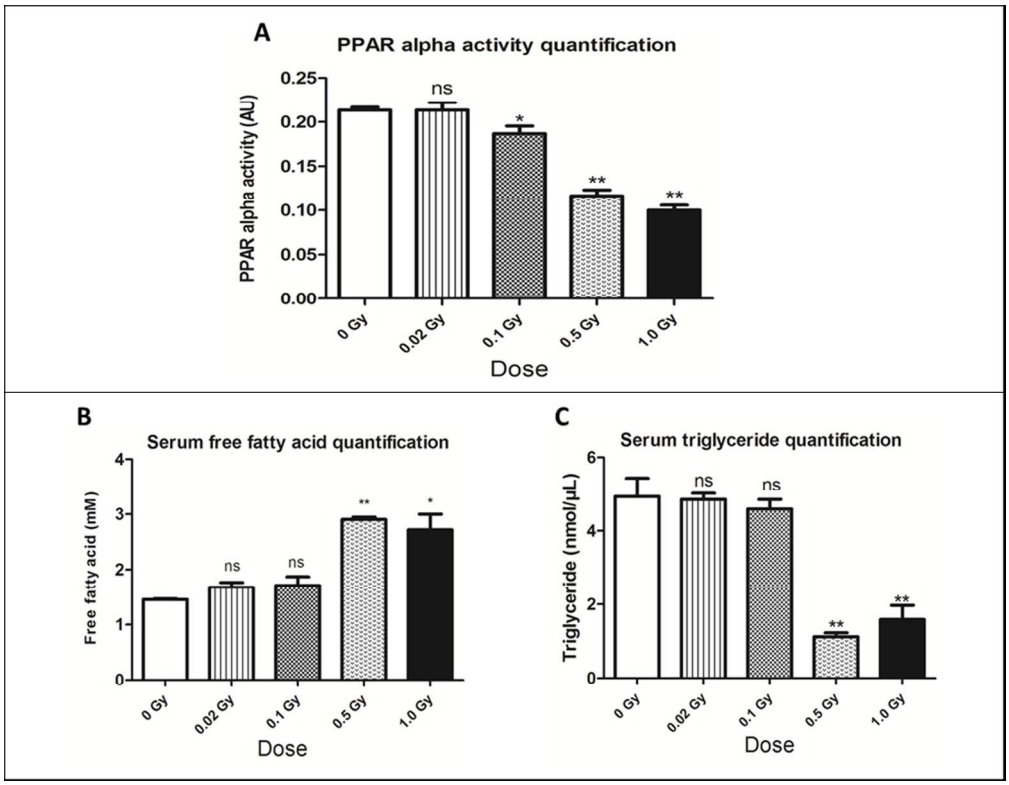

Figure 5 (A) Columns representing quantification of PPAR alpha activity assay in liver of control, 0.02, 0.1, 0.5 and 1.0 Gy samples 7 months post irradiation (AU; arbitrary unit). Columns representing quantification of triglycerides (B) and free fatty acid (C) in the serum samples of control, 0.02, 0.1, 0.5 and 1.0 Gy samples 7 month post irradiation (Unpaired Student´s t-test; *p ≤0.05; **p ≤0.01; n=3).
170x131mm (150 x 150 DPI)

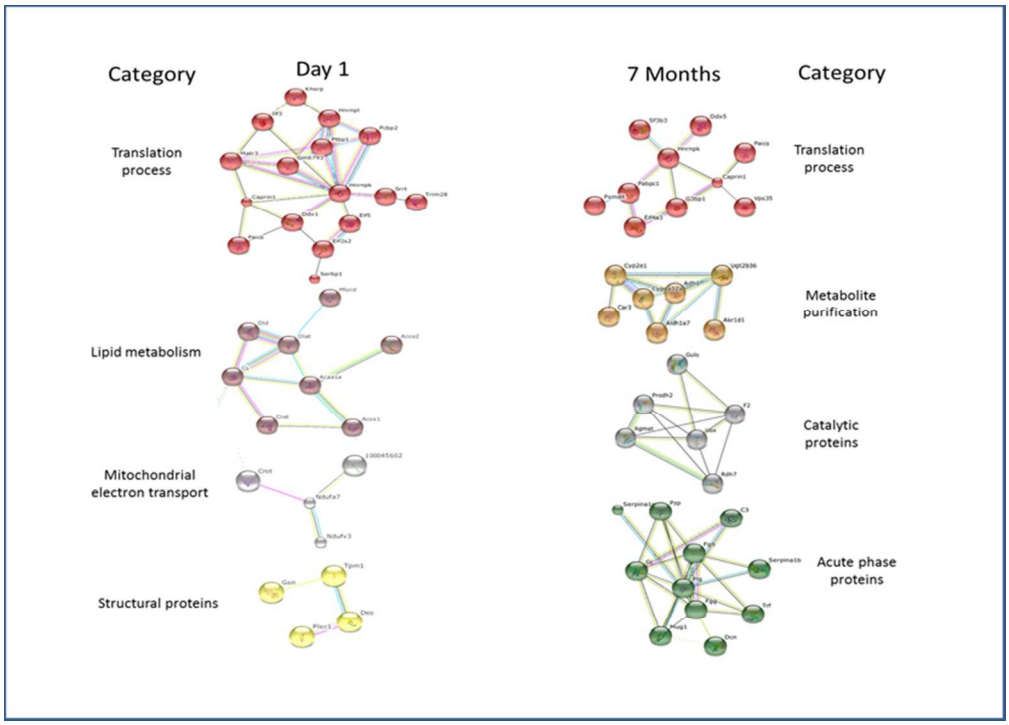

70x50mm (300 x 300 DPI)